THE JOURNAL OF PHYSICAL CHEMISTRY C

ARTICLE

pubs.acs.org/JPCC

Interaction of BrPDI, BrGly, and BrAsp with the Rutile TiO_2(110) Surface for Photovoltaic and Photocatalytic Applications: A First-Principles Study

D. Çakır,[||,†] O. Gülseren,[*,†] E. Mete,[‡] and Ş. Ellialtıoglu[§]

[†]Department of Physics, Bilkent University, Ankara 06800, Turkey

[‡]Department of Physics, Balıkesir University, Balıkesir 10145, Turkey

[§]Department of Physics, Middle East Technical University, Ankara 06531, Turkey

ABSTRACT: The adsorption of perylenediimide (PDI)-based dye compounds (BrPDI, BrGly, and BrAsp) on the defect-free unreconstructed (UR) rutile TiO_2(110) surface has been studied using total energy pseudopotential calculations based on density functional theory. All dye molecules form moderate chemical bonds with the defect-free UR rutile (110) surface in the most stable adsorption configurations. Electronic structure analysis reveals that HOMO and LUMO levels of the adsorbed dye molecules appear within the band gap and conduction band region of the UR surface, respectively. The effect of model slab thickness on interaction strength between the dye and the UR surface has also been examined. Unlike on four-layer slabs, BrGly and BrAsp molecules are dissociatively adsorbed on the three-layer slabs. Interaction between the BrPDI and partially reduced UR rutile (110) as well as the platinized UR surface has also been considered to figure out the effects of O vacancy and previously adsorbed Pt clusters on the binding, electronic, and structural properties of the dye−surface system. The BrPDI molecule prefers to bind to the O vacancy site of the partially reduced UR surface. The existence of the small Pt_n (n = 1, 3, and 5) clusters on the reduced UR surface does not significantly alter the binding strength between the surface and BrPDI.

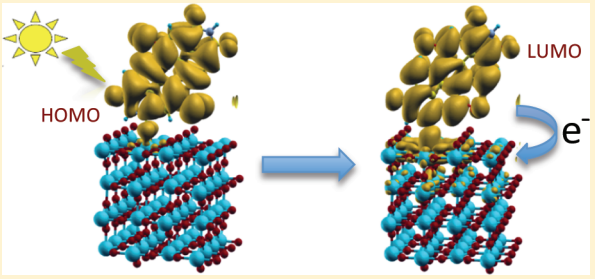

INTRODUCTION

TiO_2 is widely used in various applications because it is chemically stable in different conditions, firm under illumination, nontoxic, and relatively easy and inexpensive to produce. Most of the technology applications of TiO_2 are mainly about its optical properties such as photovoltaics and photocatalysis. TiO_2 is extensively used in dye-sensitized solar cells (DSSCs)[1,2] as an active semiconducting metal oxide. Although silicon-based solar cells are stable and capable of efficient solar energy conversion, their fabrications are rather expensive. Therefore, a growing interest is devoted to research on DSSCs.[3−5] TiO_2 is also used as a catalyst and as a catalyst support. Pt−TiO_2 and Au−TiO_2 are the most active systems studied[6,7] both theoretically and experimentally. Strong-metal-support-interaction (SMSI)[8,9] is another crucial phenomenon that affects greatly the catalytic activity on the surface. SMSI is a strong interaction observed between the small metal clusters and TiO_2 surface. A fundamental study of the interaction between the dye molecules and the defect-free unreconstructed (UR) as well as partially reduced UR and platinized UR rutile (110) surface will contribute to our understanding of the photovoltaic and photocatalytic applications of TiO_2 surfaces.

In this study, we have investigated the electronic and structural properties of UR, partially reduced UR (O deficient), and platinized UR rutile TiO_2(110) surfaces with the PDI-derived dye adsorbates, which are important for both fundamental science and technologic applications. The rutile (110) surface is the most stable surface among the other rutile and anatase surfaces. It is often considered as a model metal oxide surface for experimental as well as theoretical studies.[9,10]

METHOD

We have performed first-principles plane-wave calculations[11,12] within density functional theory (DFT)[13] using projector augmented-wave (PAW) potentials.[14,15] The exchange−correlation contributions have been treated using the generalized gradient approximation (GGA) with both PBE[16] and PW91[17] formulations. The UR−rutile (110) surface has been modeled by both three- and four-layer slabs to examine effects of thickness on binding of dye molecules on the titania surface. The three-layer slab has been mainly used for test purposes, and four-layer slab calculations will be presented in this work. Depending on the adsorption geometry, 4 × 2 and 4 × 3 slabs have been constructed. Certain criteria for the choice of supercell dimensions have been imposed. First of all, these supercells must be large enough to give the possibility to search different adsorption sites and to

Received: August 6, 2010
Revised: March 31, 2011
Published: April 14, 2011

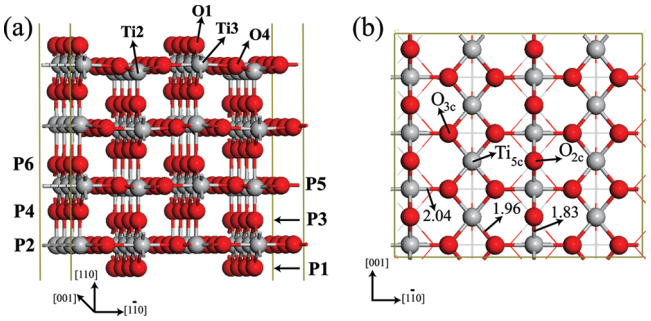

Figure 1. Side (a) and top (b) views of the defect-free unreconstructed (UR) rutile (110) surface. Interatomic distances between some of the atoms are given in Å. The bottom two layers of the UR rutile slab are considered as six atomic planes, namely, P1, P2, P3, P4, P5, and P6. The coordinations of the surface layer atoms are indicated as subscripts.

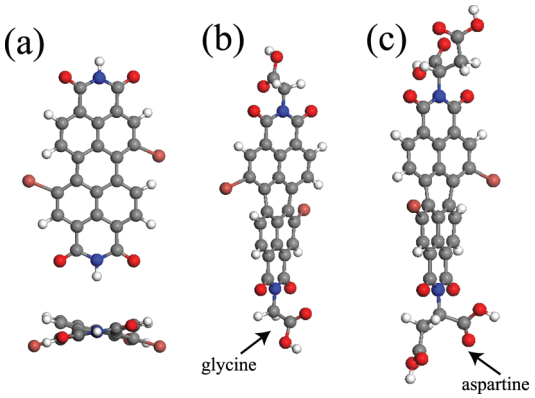

Figure 2. Calculated molecular structures of PDI-based dye molecules. Pink, white, gray, red, and blue colors represent the Br, H, C, O, and N atoms, respectively. Carboxyl groups are also shown.

prevent the interaction of the dye molecules with its periodic images. Second, they must be thick enough to reasonably reproduce most of the TiO_2 bulk properties. For the rutile (110) surface, an appropriate choice of the number of the fixed atoms or layers is crucial to obtain realistic results.[18] Therefore, several four-layer UR slab models having different numbers of fixed atomic planes at the back surface have been examined to see whether electronic properties and interaction strengths of the adsorbed dye + slab combined systems change or not. Two bottom layers can be considered as made up of six atomic planes. Descriptions of these planes (P1−P6) are depicted in Figure 1-(a). We have tested the interaction between the dye and the UR rutile surface against increasing the number of fixed atoms or layers. In all four-layer UR−dye calculations, the atoms residing in P1−P5 planes at the bottom of the slab have been fixed to their bulk positions. We allowed all the others to relax to their minimum energy configurations by using the conjugate gradient method where the total energy and Hellman−Feynman forces are minimized. The maximum force magnitude that remained on each atom has been limited to 0.06 eV/Å. For the three-layer slab, only the atoms in P1 and P2 planes were frozen to their bulk positions during the calculations. The thickness of the slab model and the number of frozen atomic planes at the back surface influence atomic relaxations as well as the relative positions of the valence band maximum (VBM) and the conduction band minimum (CBM). In agreement with the discussion of Thompson et al. on modeling the rutile TiO_2(110) surface, our tests suggest that the four-layer slab with five fixed atomic planes (P1−P5) gives well-converged results for bond lengths and binding energies.[19]

Isolated dye molecules have been relaxed in a large orthorhombic supercell such that the spacing between the adjacent dye molecules has been taken as 8 Å to prevent interaction between them. Similarly, the vacuum between the bottom of the periodic image of the back surface and the top of the adsorbed molecule has been taken to be at least 8 Å. For the Brillouin zone integrations, in the self-consistent total energy calculations, Γ point has been used. A plane-wave basis set with kinetic energy cutoff of 500 eV has been taken. For the density of states (DOS) calculations, a finer *k*-mesh has been used.

RESULTS AND DISCUSSIONS

Perylenediimide (PDI)-based dye compounds have been used in the calculations. Optimized molecular structures of these PDI-based brominated dye molecules are shown in Figure 2, in which carboxyl groups, namely, glycine (Gly) and aspartine (Asp) groups, are asymmetrically attached to the tips in the cases of BrGly and BrAsp, respectively. These molecules can be excited under visible-light illumination without undergoing molecular deformation. Time-dependent density functional theory (TDDFT) corrected HOMO−LUMO gaps for these organic dyes fall within the visible region with values 2.39, 2.38, and 2.36 eV for BrPDI, BrGly, and BrAsp, respectively, while the corresponding DFT results are all 1.45 eV. Therefore, they can be considered as potential candidates in DSSC applications which absorb photons to generate electron−hole pairs. Detailed discussions about these dye molecules have been published elsewhere.[20] In molecular design of suitable PDI-based dyes for DSSC and photocatalysis applications, the degree of dye aggregation on the titania surface, electronic coupling strength between the perylene core and the underlying surface, and the existence of multiple electron donating parts are vital parameters. PDI-based dyes can be further functionalized by replacing halogen and carboxyl group atoms with different chemical groups such as cyclohexyl groups, alkyl side chains, aromatic rings, or pyrrolidine groups.[21,22]

BrPDI Case. This dye is similar to the PTCDA (3,4,9,10-perylene-tetracarboxylicdianhydride) molecule. Two H atoms at the sides and two O atoms at the tips of planar PTCDA are substituted with two Br atoms and two NH molecules, respectively. As a result of the repulsive interaction between Br and its nearest-neighbor hydrogen, the perylene skeleton of the BrPDI is slightly twisted. Figure 2 shows the calculated optimized structure of BrPDI. Figure 3(a) presents the adsorption of BrPDI dye on the 4 × 2 four-layer UR surface. This surface is large enough to study particular adsorption modes in which the perylene part of the dye is perpendicular to the UR surface. For the most stable adsorption case, the O atom of the dye binds to the 5-fold coordinated Ti atom on the UR surface with an interatomic distance of 2.04 Å. Moreover, two H atoms of dye interact with the two 2-fold coordinated bridge O atoms. Interatomic distances in these two H−O bonds are 2.01 and 1.83 Å, respectively. Binding energy E_b of adsorbed dye on the UR surface has been calculated in terms of the total energy of the clean UR surface E_T[slab], free dye E_T[dye], and dye on the slab E_T[slab + dye] through the following relation

$$E_b = E_T[\text{slab}] + E_T[\text{dye}] - E_T[\text{slab} + \text{dye}]$$

dx.doi.org/10.1021/jp107428t |*J. Phys. Chem. C* 2011, 115, 9220–9226

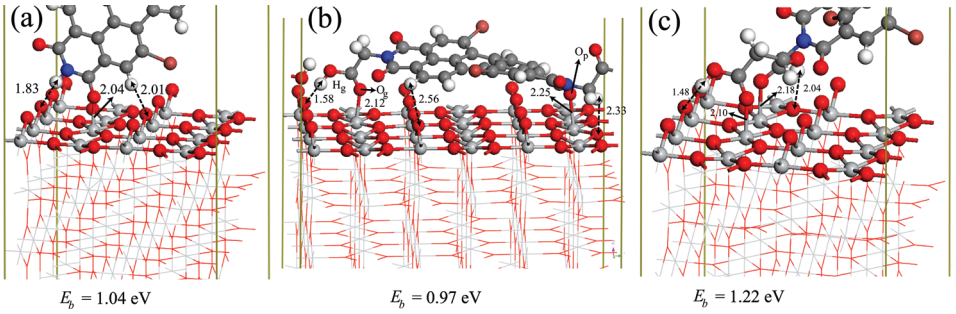

Figure 3. Fully optimized geometry of the most stable adsorption modes of (a) UR−BrPDI, (b) UR−BrGly, and (c) UR−BrAsp. The 4 × 2 UR slab has been constructed for the BrPDI and BrAsp dyes. For the BrGly molecule, calculations have been done on the 4 × 3 UR rutile surface. Only the bonded part of the molecules is shown. Detailed structures of dyes are displayed in Figure 2. Binding energy (E_b) is given for each adsorption case. Interatomic distance (in Å) between some of the atoms is shown.

The value of E_b for the lowest-energy adsorption mode of BrPDI is 1.04 eV.

When the perylene part of the dye is parallel to the UR surface, the 4 × 2 cell is not large enough to study this adsorption mode. As a result, we have constructed the 6 × 2 cell. To reduce the computational costs and study the effects of thickness on the interaction between the UR surface and BrPDI dye, the 6 × 2 UR slab consisted of three layers. Three main configurations at which dye is parallel to the UR surface have been built. In the first one, the longer part of the dyes is along the [001] direction of the UR surface. We have rotated the first structure by 90° to obtain the second one. In this case, the longer part of the dye is oriented along the $[1\bar{1}0]$ direction. The last configuration is the mixing of the first two cases. Dye is oriented along the diagonal of the UR surface. We have started with three initial structures. One of them is energetically the most stable adsorption structure of the 4 × 2 four-layer slab case. It is possible to construct a large number of initial geometries; however, one can reduce the number of possibilities by using certain basic rules. We know that O atoms on the surface are negatively charged. Surface Ti atoms and H atoms of the molecule do not prefer to bind to each other. By using these simple electrostatic arguments, we have formed two initial structures in which the molecule is parallel to the UR surface. The ground state adsorption geometry in both slab thicknesses is the same. E_b for the three-layer slab case is 1.11 eV, and this binding energy is greater than that for the four-layer slab.

BrGly Case. BrGly contains two glycines as carboxyl groups. The glycine ligand and one of the perylene O atoms anchor BrGly to the UR rutile (110) surface. Figure 3(b) presents the optimized adsorption geometry of BrGly on the UR surface for the energetically most stable structure. Because of the positions of the glycine groups with respect to the middle part of the dye, the perylene part is parallel to the UR surface in the most stable adsorption structure. Therefore, the 4 × 3 slab has been used for the simulation of this adsorption mode. Dye makes two contacts with the UR titania surface. The anchor group O (O_g) atom interacts more strongly with the UR surface Ti atoms compared to the perylene O_p atom. The interatomic distance between the UR surface Ti and the O_g (O_p) atom is 2.12 (2.25) Å. H atoms at the edge of the perylene core and glycine H (H_g) atoms interact with the UR surface bridge O atoms. The distance between the H_g and its nearest bridge UR surface O is 1.58 Å. The other ligand does not participate in the binding. Dye is molecularly adsorbed by the UR surface with an E_b of 0.97 eV.

BrAsp Case. In this dye, the anchor group is aspartine. The BrAsp sticks to the UR surface through one of its carboxylic groups. Two O atoms of the anchor group bind to Ti atoms with an average interatomic distance of 2.14 Å. Moreover, H atoms of aspartine interact with bridge and basal O atoms giving rise to increased interaction between the dye and the UR surface. E_b of the most stable adsorption mode is 1.22 eV, and this corresponds to a molecular adsorption.

Binding energy of BrGly is smaller than that of BrPDI and BrAsp dyes on the UR surface. In the BrGly case, the perylene skeleton is parallel to the UR surface, and this situation enhances the repulsive interaction between the surface and the dye. In addition, bending of BrGly through its molecular axis over the surface weakens the binding. In the dye−surface systems, binding mainly results from the Ti−O interactions. BrGly and BrAsp dyes are dissociatively adsorbed on the three-layer UR slab. The O−H bond in the ligand part breaks, and the H atom of glycine and aspartine anchor groups binds to the bridge O atom on the UR surface. All dyes bind more strongly to the three-layer UR slab. For the most stable adsorption structure of BrAsp on the three-layer UR slab, E_b is 1.76 eV. We have shown that molecular adsorption of the dyes is favored on the UR rutile surface with at least the four-layer thick slab model.

For efficient photovoltaic and photocatalytic applications of dye−TiO_2 surface systems, it is crucial to use a large part of the solar spectrum. However, TiO_2 absorbs the ultraviolet (UV) portion of the spectrum, which is only about 3% of the whole. In the dye−surface systems, dye is responsible for the optical processes which take place in the visible region. In DSSC devices, dye is excited by photons, and as a result electron−hole pairs are generated by this illumination. Generated electrons in the excited states of the dye must be injected to the conduction band of a semiconductor, and this injection has to be very fast to prevent recombination, the reduction of the oxidized dye. Therefore, the position of HOMO−LUMO levels of the dyes with respect to VB and CB edges of TiO_2 is very crucial. For an efficient solar cell, the HOMO level produces occupied levels inside the gap region, and LUMO is well localized across the CB of the slab.

Figure 4 shows the partial density of states (PDOS) of the surface + dye systems for the most stable adsorption modes. We notice that all adsorbed dyes induce occupied states inside the band gap of UR rutile. Moreover, LUMO levels of these molecules fall inside the CB of the UR slab. Carboxyl groups do not contribute to the HOMO nor to the LUMO levels of the free dyes. Therefore, electronic coupling strength between the

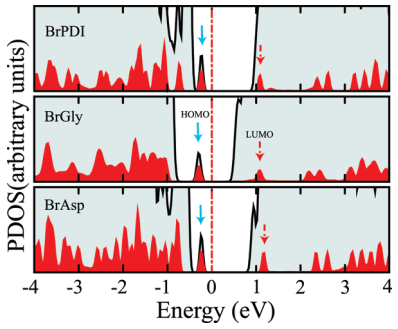

Figure 4. Projected density of states (PDOS) of (a) BrPDI, (b) BrGly, and (c) BrAsp. DOS of the total system and adsorbed dye are represented by gray and red colors, respectively. The Fermi level is shown by the red dotted−dashed line. Cyan and dotted−dashed red arrows mark the position of HOMO and LUMO levels of adsorbed dye molecules. We have used the Gaussian function with a smearing parameter of 0.05 eV and $3 \times 2 \times 1$ k-points mesh in PDOS calculations.

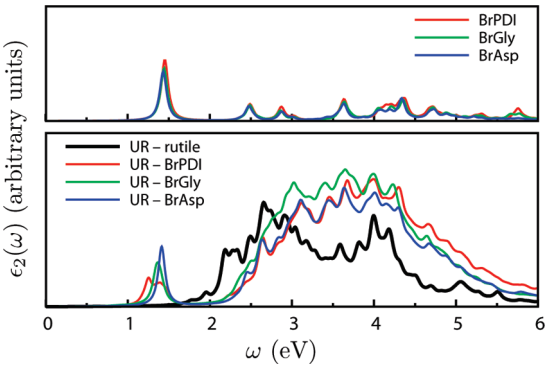

Figure 5. Absorption spectra of isolated dye molecules (top panel) and those of adsorbed dye on unreconstructed (lower panel) rutile (110) surfaces compared also with the clean surface for both surfaces (black solid curves).

perylene core and TiO_2 influences the performance of the DSSC. For the BrPDI and BrGly adsorption, there is a significant coupling between these dyes and the underlying UR surface. As a result, it is expected that the electron injection process from the BrPDI and BrGly excited singlet states to the CB of the UR surface is faster than those of BrAsp. Slow electron injection rate means low power conversion efficiency in the DSSC devices.

We obtained the optical absorption spectra by evaluating dipole matrix elements between occupied and unoccupied states for each of the cases. Figure 5 shows the calculated $\varepsilon_2(\omega)$ for isolated dye molecules and bare rutile $TiO_2(110)$ surfaces as well as for the dye−surface composite systems. All these molecules possess strong optical peaks at 1.45 eV corresponding to the gaps which are underestimated by DFT. For the bare UR surface (black solid curve in the lower panel), absorption starts after about 1.6 eV. The comparison of the first peaks of the BrAsp−UR system and the isolated BrAsp shows that these peaks are consistent with the HOMO−LUMO gap of the dye. Similarly, the first peaks of BrPDI and BrGly on the UR surface are slightly red-shifted isolated dye peaks. The TDDFT treatment for the composite systems is still computationally demanding. Moreover, one has to include the local field effects with correct electron self-energy to perform TDDFT calculations for such periodic systems. Although DFT is a ground state theory which is not suited to get absorption spectra, it still gives a reasonable description of the photoexcitation for these particular dye−UR systems except the position of the first peaks. In fact, we have previously showed that the positions of these peaks are well predicted to be at around 520 nm by TDDFT correction[20] in good agreement with the experimental findings.[23,24] The dispersion of the absorption peaks for these dye compounds is influenced by their molecular structures, adsorption geometries, and factors like the ambient temperature and coupling to environment.[23] Therefore, the main absorption peaks for BrPDI, BrGly, and BrAsp are characterized by a transition between the HOMO−LUMO levels. These optical transitions agree well with the photoexcitation process in a DSSC application. Moreover, the dye LUMO levels are positioned well inside the CB of the semiconductor which allows charge injection to the substrate.

BrPDI Dye on the Partially Reduced UR Rutile (110) Surface. Oxygen vacancy is one of the main point defects on the rutile (110) surface. It significantly influences the physical and chemical properties of metal oxide surfaces[9] and can act as the preferential adsorption site for adatoms or admolecules. Formation of oxygen vacancy at the bridge site gives rise to two excess electrons. Ti^{3+} ions and localized band gap states form upon reduction of the surface. These gap states are mainly of Ti 3d character.[25,26] There is a disagreement among the various first-principles calculations about the distribution of these excess charges. Different exchange and correlation (XC) potentials give very conflicting results. According to standard DFT using LDA or GGA, excess charges populate the bottom of the conduction band, which gives the delocalization of these excess charges over several surface and subsurface layers.[27,28] However, hybrid functionals such as B3LYP predict localization of defect charge over two specific surface Ti sites.[29] It is known that DFT fails to describe strongly correlated systems. The DFT+U approach provides a reasonable description of the electronic and geometric structure of the reduced surface, which is consistent with some experiments. However, in a recent experiment by using the resonant photoelectron diffraction technique,[30] it has been shown that the defect charge is distributed over several surface and subsurface Ti sites. These results are consistent with DFT calculations which have predicted a delocalization of the defect charge. DFT theory based on Kohn−Sham orbitals predicts an underestimated band gap. However, it generally predicts adsorbate binding energy correctly. In this work, we have also examined the interaction between the BrPDI and partially reduced 4×2 rutile (110) surface possessing single O vacancy. We have tried to obtain qualitative results for the binding of the dye on reduced surface. Single O vacancy has been obtained by removing a bridging oxygen from the 4×2 surface. The resulting partially reduced surface has a ferromagnetic ground state. The induced magnetic moment upon formation of single O vacancy is 1.77 μ_B. In contrast to this large magnetic moment, the energy difference between the ferromagnetic and nonmagnetic solutions is 20 meV. As a result of O vacancy, the structure of the surface at the vicinity of vacancy is disturbed. On reduced surfaces, vacancies are very reactive sites. In the construction of initial structures for the BrPDI−surface system, this argument has been adopted. During the calculations, the effect of spin polarization has been ignored. For the most stable adsorption mode, the O atom of BrPDI prefers to occupy the position of the vacancy (see Figure 6(a)). Two H atoms of the dye interact with the bridge and basal O atoms. E_b of this adsorption mode is 1.22 eV, which is

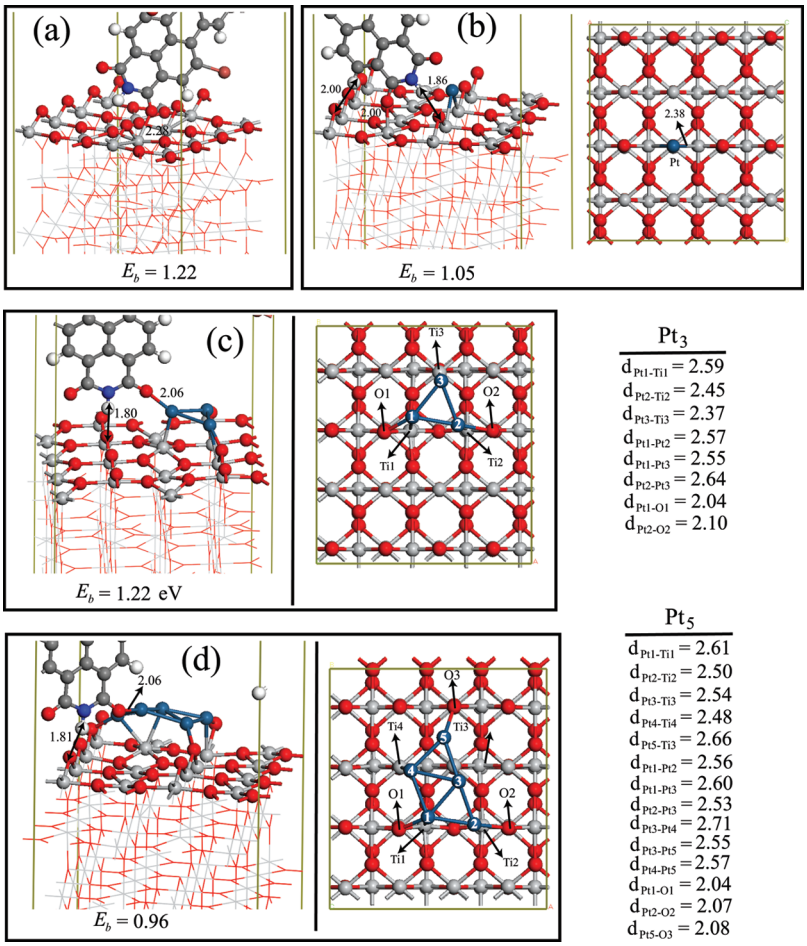

Figure 6. Fully optimized geometry of the most stable adsorption modes of BrPDI on (a) partially reduced, (b) Pt−surface, (c) Pt_3−surface, and (d) Pt_5−surface. Top view of the ground state structure of the Pt monomer, Pt_3, and Pt_5 clusters adsorbed on the partially reduced 4 × 2 rutile (110) surface is also represented. Binding energy (E_b) is given for each adsorption case in eV. Interatomic distance (in Å) between some of the atoms is shown.

greater than the E_b of BrPDI on the defect-free UR rutile (110) surface (see Figure 3).

BrPDI Dye on Platinized UR Rutile (110) Surface. Photoreduction of CO_2 under UV and visible light has been tested over the dye (brominated PDI derivatives: BrGly and BrAsp) sensitized, Pt-promoted thin and thick films of TiO_2 by Ozcan et al.[31] Pure and Pt-containing TiO_2 films are inactive under visible light. These films are activated by the adsorbed organic dye sensitizers. Furthermore, we have also studied the interaction of BrPDI with the platinized rutile surface as a prototype of the dye−Pt−surface system. For this surface, three cases have been considered. For the first one, the single Pt atom is adsorbed by the surface at the vacancy site. A three-atom cluster is formed at the vicinity of the vacancy site for the second case. Finally, a five-atom Pt cluster on this surface is considered. Ground state structures of Pt_n clusters (n = 1, 3, and 5) adsorbed on the partially reduced 4 × 2 rutile (110) surface are shown in Figure 6. It is noticed that the interatomic distances in Pt−Ti and Pt−Pt bonds increase as the coordination number of Pt atoms increases. Binding energy per Pt atom on the partially reduced surface has been calculated in the following way

$$E_b = (E[\text{slab}] + nE[\text{Pt}] - E[\text{slab} + \text{Pt}_n])/n$$

In this formula, E[slab], E[Pt], and E[slab + Pt_n] are the total energies of the bare slab, free Pt atom, and the fully relaxed slab + Pt system. Here, n represents the number of Pt atoms adsorbed on the surface. The values of E_b for monomer, trimer, and pentamer clusters are 3.15, 3.66, and 3.83 eV, respectively. The ground state structure of the adsorbed Pt_3 cluster has triangular geometry, and two Pt atoms are adsorbed at the vacancy site of the surface. The adsorbed Pt_5 cluster has a planar ground state structure on the reduced surface. Pt_3 and Pt_5 clusters have been constructed by repeatedly adding a single Pt atom to a smaller cluster and allowing the structure to relax on each step. We have performed a systematic search to find the lowest energy structure of these small clusters on the titania surface. Inclusion of spin polarization effects on the calculations was tested and found to be negligible. Figure 7 shows the partial density of states for the Pt_n−surface systems before and after the interaction with BrPDI. The analysis of the density of states reveals that the Pt_n−surface system becomes metallic for n = 3 and 5. Metal-induced states are observed in the band gap of surface for the Pt monomer case. Because of these states, adsorption of a single Pt atom lowers the optical threshold of the rutile (110) surface. Figure 6 shows the optimized structure of BrPDI adsorbed on platinized rutile (110) surface (Pt_n−surface, where n = 1, 3, and 5). For the interaction between the dye and Pt_1−surface system, the most energetic adsorption site is the same as the adsorption of BrPDI on the defect-free UR rutile surface. Dye molecule does not interact with the previously adsorbed Pt atom. The calculated molecular binding energy is 1.05 eV for this case. In contrast to

dx.doi.org/10.1021/jp107428t |J. Phys. Chem. C 2011, 115, 9220–9226

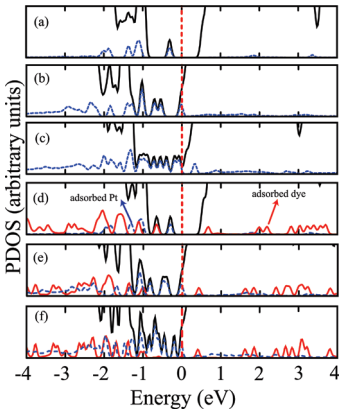

Figure 7. Projected density of states (PDOS) of (a) Pt monomer, (b) Pt_3, and (c) Pt_5 clusters adsorbed on the partially reduced 4 × 2 rutile (110) surface. PDOS of BrPDI adsorbed on (d) Pt−surface, (e) Pt_3−surface, and (f) Pt_5−surface. DOS of total system, adsorbed dye, and Pt atoms are represented by black, red, and blue colors, respectively. Fermi level is shown by the red dotted−dashed line. We have used Gaussian function with a smearing parameter of 0.05 eV and 3 × 2 × 1 *k*-points mesh in the PDOS calculations.

the Pt_1−surface system, adsorbed Pt clusters contribute to the binding of dye on the surface in the cases of Pt_3 and Pt_5 clusters. In both cluster cases, the O atom of BrPDI binds to a particular Pt atom of the clusters with an average interatomic distance of 2.04 Å. In Pt-oxides, Pt−O bond length is about 2.0 Å. In addition to Pt−O bonds, the H atom at the tip of the dye molecule interacts with a 2-fold coordinated bridging O atom at the surface in the presence of both Pt_3 and Pt_5 clusters. The interatomic distance between these two interacting atoms is about 1.80 Å. We have also calculated the binding energy of BrPDI on the Pt_n−UR surfaces which are 1.22 for $n = 3$ and 0.96 eV for $n = 5$ clusters. In principle, one might expect a Schottky barrier formation at the Pt/TiO_2 interface; hence, electrons cannot easily transfer from Pt to TiO_2. However, here, we have only considered very small Pt_n clusters adsorbed on the surface. For all Pt_n (n = 1, 3, and 5) cases, the dye brings an occupied state localized in the gap which derives from the HOMO level of the adsorbed dye. Moreover, the LUMO level is well localized within the CB of the surface. Unlike the optimized BrPDI−Pt_1−UR surface system, it is hard to inject an excited electron of the dye into the CB of the underlying surface in the case of Pt_3 and Pt_5. In these cluster cases, dye interacts with surface through its H atom which has no contribution to the formation of LUMO of the dye. The generated charge eventually transfers to the Pt_3 or Pt_5 clusters. In the dye−Pt_n−surface system, first, the dye is excited by the visible light. Generated charge may be transferred to the Pt clusters by the following two ways: (1) Dye→surface→Pt_n and (2) Dye→Pt_n. In the first case, we have multiple charge transfer mechanisms which can be observed in the case of dye−Pt_1−surface. When the charge reaches the Pt cluster, it can be used in the catalytic process, which takes place on a cluster. In this way, visible-light photocatalysis is obtained by using dyes as light-harvesting molecules. We considered simple dye−cluster−surface systems with rather small Pt clusters. However, this work provides a fundamental understanding for the photocatalysis applications of the dye−Pt-promoted−titania surfaces.

CONCLUSION

In conclusion, the adsorption of BrPDI, BrGly, and BrAsp dye molecules on defect-free UR rutile (110) surfaces has been investigated. Dyes bind to the UR surface strongly. As a result of interaction between the dye and UR surface, an optical response of the combined system is adapted to visible light. Regardless of the type of dye molecules and surfaces, HOMO and LUMO levels of adsorbed dye appear within the gap and conduction band region of the UR surface, respectively. We have performed the calculations on both three- and four-layer thick UR slabs. It is observed that the computed binding energies of the dyes are dependent on the thickness of the slab. We have also discussed the interaction of the BrPDI molecule with the partially reduced and platinized UR rutile (110) surfaces. For the reduced UR surface, dye prefers to bind to the O vacancy site. Adsorption of Pt atoms on the partially reduced UR surface greatly influences the electronic properties of the rutile (110) surface.

AUTHOR INFORMATION

Corresponding Author

*E-mail: gulseren@fen.bilkent.edu.tr.

Present Addresses

[||]Faculty of Science and Technology and MESA[+] Institute for Nanotechnology, University of Twente, P.O. Box 217, 7500 AE Enschede, The Netherlands.

ACKNOWLEDGMENT

EM and ŞE acknowledge the partial support from TÜB İTAK, The Scientific and Technological Research Council of Turkey (Grant no: TBAG 107T560). OG acknowledges the support of Turkish Academy of Sciences, TÜBA. Computing resources used in this work were provided by the National Center for High Performance Computing of Turkey (UYBHM) under grant number 10362008.

REFERENCES

(1) O'Regan, B.; Grätzel, M. *Nature* **1991**, *353*, 737–740.
(2) Grätzel, M. *Nature* **2001**, *414*, 338–344.
(3) Li, B.; Wang, L.; Kang, B.; Wang, P.; Qiu, Y. *Sol. Energy Mater. Sol. Cells* **2006**, *90*, 549–573.
(4) Çakır, D.; Gülseren, O.; Mete, E.; Ellialtıoğlu, Ş. *Phys. Rev. B* **2009**, *80*, 035431.
(5) Mora, G. K.; Varghesea, O. K.; Paulosea, M.; Shankara, K.; Grimes, C. A. *Sol. Energy Mater. Sol. Cells* **2006**, *90*, 2011–2075.
(6) Mete, E.; Uner, D.; Gülseren, O.; Ellialtıoğlu, Ş. *Phys. Rev. B* **2009**, *79*, 125418.
(7) Mete, E.; Gülseren, O.; Ellialtıoğlu, Ş. *Phys. Rev. B* **2009**, *80*, 035422.
(8) Tauster, S. J.; Fung, S. C.; Garten, R. L. *J. Am. Chem. Soc.* **1978**, *100*, 170–175.
(9) Diebold, U. *Surf. Sci. Rep.* **2003**, *48*, 53–229.
(10) Chen, X.; Mao, S. S. *Chem. Rev.* **2007**, *107*, 2891–2959.
(11) Payne, M. C.; Teter, M. P.; Allen, D. C.; Arias, T. A.; Joannopoulos, J. D. *Rev. Mod. Phys.* **1992**, *64*, 1045–1097.
(12) Computations have been carried out with the VASP software: Kresse, G.; Hafner, J. *Phys. Rev. B* **1993**, *47*, 558–561. Kresse, G.; Furthmüller, J. *Phys. Rev. B* **1996**, *54*, 11169–11186.
(13) Kohn, W.; Sham, L. J. *Phys. Rev.* **1965**, *140*, A1133–A1138. Hohenberg, P.; Kohn, W. *Phys. Rev.* **1964**, *136*, B864–B871.
(14) Blöchl, P. E. *Phys. Rev. B* **1994**, *50*, 17953–17979.
(15) Kresse, G.; Joubert, D. *Phys. Rev. B* **1999**, *59*, 1758–1775.
(16) Perdew, J. P.; Burke, K.; Ernzerhof, M. *Phys. Rev. Lett.* **1996**, *77*, 3865–3868.

(17) Perdew, J. P.; Chevary, J. A.; Vosko, S. H.; Jackson, K. A.; Pederson, M. R.; Singh, D. J.; Fiolhais, C. *Phys. Rev. B* **1992**, *46*, 6671–6687.
(18) Hameeuw, K. J.; Cantele, G.; Ninno, D.; Trani, F.; Iadonisi, G. *J. Chem. Phys.* **2006**, *124*, 024708.
(19) Thompson, S. J.; Lewis, S. P. *Phys. Rev. B* **2006**, *73*, 073403.
(20) Mete, E.; Uner, D.; Çakmak, M.; Gülseren, O.; Ellialtıoğlu, Ş. *J. Phys. Chem. C* **2007**, *111*, 7539–7547.
(21) Zafer, C.; Kus, M.; Turkmen, G.; Dincalp, H.; Demic, S.; Kuban, B.; Teoman, Y.; Icli, S. *Sol. Energy Mater. Sol. Cells* **2007**, *91*, 427–431.
(22) Shibano, Y.; Umeyama, T.; Matano, Y.; Imahori, H. *Org. Lett.* **2007**, *9*, 1971–1974.
(23) Alvino, A; Franceschin, M.; Cefaro, C.; Borioni, S.; Ortaggi, G.; Bianco, A. *Tetrahedron* **2007**, *63*, 7858–7865.
(24) Shin, W. S.; Jeong, H.-H.; Kim, M.-K.; Jin, S.-H.; Kim, M.-R.; Lee, J.-K.; Lee, J. W.; Gal, Y.-S. *J. Mater. Chem.* **2006**, *16*, 384–390.
(25) Zhang, Z.; Jeng, S.-P.; Henrich, V. E. *Phys. Rev. B* **1991**, *43*, 12004–12011.
(26) Le Fèvre, P.; Danger, J.; Magnan, H.; Chandesris, D.; Jupille, J.; Bourgeois, S.; Arrio, M.-A.; Gotter, R.; Verdini, A.; Morgante, A. *Phys. Rev. B* **2004**, *69*, 155421.
(27) Paxton, A. T.; Thiên-Nga, L. *Phys. Rev. B* **1998**, *57*, 1579–1584.
(28) Pillay, D.; Hwang, G. S. *Phys. Rev. B* **2005**, *72*, 205422.
(29) Di Valentin, C.; Pacchioni, G.; Selloni, A. *Phys. Rev. Lett.* **2006**, *97*, 166803.
(30) Krüger, P.; Bourgeois, S.; Domenichini, B.; Magnan, H.; Chandesris, D.; LeFèvre, P.; Flank, A. M.; Jupille, J.; Floreano, L.; Cossaro, A.; Verdini, A.; Morgante, A. *Phys. Rev. Lett.* **2008**, *100*, 055501.
(31) Ozcan, O.; Yukruk, F.; Akkaya, E. U.; Uner, D. *Appl. Catal. B: Environ.* **2007**, *71*, 291–297.